EARTHQUAKE ENGINEERING AND STRUCTURAL DYNAMICS
Earthquake Engng Struct. Dyn. 2007; **36**:13–33
Published online 10 July 2006 in Wiley InterScience (www.interscience.wiley.com). DOI: 10.1002/eqe.607

Linear models with nearly frequency independent complex stiffness leading to causal behaviour in time domain

G. B. Muravskii*, †

Faculty of Civil Engineering, Technion—Israel Institute of Technology, Haifa 32000, Israel

SUMMARY

In the paper, several causal linear models leading to nearly frequency independent complex stiffness are studied in time and frequency domains. Along with Biot model other three hereditary models are introduced into analysis. They all ensure practical constancy for damping properties but have limitations concerned with an increase in the real part of complex stiffness of corresponding material elements, as frequency grows. A new suggested method deals with given mechanical system as a whole: the imaginary part of the system compliance is constructed assuming that all elements have constant stiffness (with a modification for imaginary parts near zero frequency) and further the imaginary part of the system is used directly for studying transient vibrations supposing causality of the given mechanical system. The corresponding real part (not needed in the transient response analysis) is determined by Hilbert transformation. Examples relating to systems with one, two and infinite (shear beam) degrees of freedom are carried out for five compared models, allowing to reveal advantages and shortcomings of the models.

Received 12 December 2005; Revised 27 May 2006; Accepted 31 May 2006

KEY WORDS: frequency independent damping; causality; hereditary models; Hilbert transformation; shear beam

INTRODUCTION

The well-known concept of a ‘spring’ having frequency independent complex stiffness (ideal hysteretic model) was introduced into theory of vibration by Theodorsen and Garrick [1]. It works well in frequency domain when one deals with harmonic or periodic steady-state processes. Difficulties emerge when going to the area of transient vibrations. Fraijs de Veubeke [2], Caughey [3] and Crandall [4] had shown independently that the ‘spring’ has non-causal behaviour, and as result the corresponding mechanical system begins to move before a load application.

*Correspondence to: G. B. Muravskii, Faculty of Civil Engineering, Technion—Israel Institute of Technology, Haifa 32000, Israel.
†E-mail: gmuravsk@tx.technion.ac.il

Nevertheless, in the last two decades the ideal hysteretic model attracted wide attention of investigators, which concerned mostly with constructing a transient response for a mechanical system containing ideal hysteretic elements. Gaul *et al*. [5] investigated the initial conditions corresponding to the non-causality. Milne [6] studied the impulse-response function of a simple oscillator with the ideal hysteretic 'spring'. Inaudi and Kelly [7], Chen and You [8, 9] considered the application of Hilbert transform operator to time-domain representation for the model.

A formulation of transient behaviour of a system based on differential equations with complex-valued coefficients and analytical input was developed by Inaudi and Makris [10, 11]. In papers by Makris [12, 13], the question of building a causal model having a constant (for the positive frequency domain) damping part is addressed. Because of discontinuity of the imaginary part of the complex stiffness when going to negative frequencies, the corresponding real part tends to infinity nearby zero frequency. Makris [13] showed that the constructed model can be considered as a limit for Biot model [3, 14]. This model, ensuring practically independent damping at a required frequency interval, was investigated recently in papers by Makris and Zhang [15], Spanos and Tsavachidis [16], Muscolino *et al*. [17]. In the suggested paper, the Biot model along with other hereditary models is studied. Because of an increase of stiffness with the growth of frequency, these models can lead to significant errors when damping parameters are large as in case of soil foundations. As developed in the paper method of constructing a causal model with nearly constant stiffness and damping characteristics based on consideration of the system as the whole, extend the area of applicability of the hereditary models. Also the equivalent viscous model is considered in the paper as a reference model. Actually, this model is an appropriate choice if we deal with a single-degree of freedom mechanical system (SDoF) or with multi-degree of freedom systems (MDoF) whose damping and stiffness properties have nearly identical distribution. In the case of MDoF, separate modes of vibration are provided with a suitable amount of damping [18, 19]. The assumption that the system with damping has the same natural modes as the corresponding undamped system, may not be appropriate in some cases (see Reference [19]). This is demonstrated also below in this paper.

Note that strictly constant complex stiffness (with causality) can be achieved with the help of non-linear models [20, 21]. The quasi hysteretic model [20] and hysteretic model with linear backbone curve [21] seem to be a suitable alternative to the ideal hysteretic model when dealing in the time domain.

APPLICATION OF HEREDITARY LINEAR MODELS FOR DESCRIPTION NEARLY CONSTANT COMPLEX STIFFNESS

The one of linear models with nearly frequency independent damping is Biot model [3, 14] having the following relationship between force F and displacement x (assuming the loading begins at moment $t=0$):

$$F = k\left[x + \eta \int_0^t G(\varepsilon_1(t-s))\frac{\mathrm{d}x}{\mathrm{d}s}\,\mathrm{d}s\right] \tag{1}$$

where the exponential integral is used as the kernel:

$$G(u) = -\frac{2}{\pi}E_i(-u) = \frac{2}{\pi}\int_u^\infty \frac{e^{-\xi}}{\xi}\,\mathrm{d}\xi \tag{2}$$

DOI: 10.1002/eqe

Coefficients k and η are stiffness (static) and damping parameter (loss factor), respectively; parameter ε_1, which can be considered as a reference circular frequency, represents a scale factor. It is advisable to turn to non-dimensional time using the first natural (without accounting on damping) circular frequency ω_1 of the mechanical system, a part of which the considered hereditary element is

$$\tau = \omega_1 t \tag{3}$$

Equation (1) takes the form

$$F = k\left[x + \eta \int_0^{\tau} G(\varepsilon(\tau - s))\frac{\mathrm{d}x}{\mathrm{d}s}\,\mathrm{d}s\right] \tag{4}$$

where F and x are understood as functions of the non-dimensional time; $\varepsilon = \varepsilon_1/\omega_1$ is the non-dimensional scale parameter. For a force of the form $F = F_0 \exp(\mathrm{i}z\tau)$, where $z = \omega/\omega_1$ is the non-dimensional circular frequency, the displacements take the similar form when $\tau \to \infty$: $x = x_0 \exp(\mathrm{i}z\tau)$ which results in the following relation for amplitudes F_0, x_0:

$$F_0 = k^* x_0 = k(a + \mathrm{i}b)x_0 \tag{5}$$

$$a = 1 + \eta z \int_0^{\infty} G(\varepsilon u)\sin(zu)\,\mathrm{d}u = 1 - \frac{2}{\pi}\eta z \int_0^{\infty} E_i(-\varepsilon u)\sin(zu)\,\mathrm{d}u = 1 + \frac{\eta}{\pi}\ln(1 + \widetilde{z}^2) \tag{6}$$

$$b = \eta z \int_0^{\infty} G(\varepsilon u)\cos(zu)\,\mathrm{d}u = -\frac{2}{\pi}\eta z \int_0^{\infty} E_i(-\varepsilon u)\cos(zu)\,\mathrm{d}u = \frac{2\eta}{\pi}\arctan(\widetilde{z}) \tag{7}$$

where $\widetilde{z} = z/\varepsilon$. Analogous results can be obtained using arbitrary positive kernels having a logarithmic singularity at origin and decreasing with $t \to \infty$. For example, the kernel

$$G(u) = \frac{2}{\pi}K_0(u) \tag{8}$$

where $K_0(u)$ is modified Bessel function leads to the following equations (see Reference [22]):

$$a = 1 + \eta z \frac{2}{\pi}\int_0^{\infty} K_0(\varepsilon u)\sin(zu)\,\mathrm{d}u = 1 + \frac{2\eta\widetilde{z}}{\pi\sqrt{1 + \widetilde{z}^2}}\ln\left[\widetilde{z} + \sqrt{1 + \widetilde{z}^2}\right] \tag{9}$$

$$b = \eta z \frac{2}{\pi}\int_0^{\infty} K_0(\varepsilon u)\cos(zu)\,\mathrm{d}u = \frac{\eta\widetilde{z}}{\sqrt{1 + \widetilde{z}^2}} \tag{10}$$

The behaviour of a and b in frequency domain is similar to that corresponding to Equations (6) and (7). When implementing straight integrations in time domain, simpler kernels seem to be more desirable. Consider for example the kernel

$$G(u) = \frac{1}{\pi}\ln\frac{1 + u^2}{u^2} \tag{11}$$

DOI: 10.1002/eqe

Using integration by parts this leads to the following equations for a and b:

$$a = 1 + \frac{2\eta}{\pi}\left[\boldsymbol{C} + \ln(\widetilde{z}) + \int_0^\infty \frac{u\cos(\widetilde{z}u)}{1+u^2}\,\mathrm{d}u\right]$$

$$= 1 + \frac{2\eta}{\pi}\left[\boldsymbol{C} + \ln(\widetilde{z}) + \mathrm{Shi}(\widetilde{z})\sinh(\widetilde{z}) - \mathrm{Chi}(\widetilde{z})\cosh(\widetilde{z})\right] \tag{12}$$

$$b = \frac{2\eta}{\pi}\int_0^\infty \frac{\sin(\widetilde{z}u)}{u(1+u^2)}\,\mathrm{d}u = \eta[1 - \exp(-\widetilde{z})] \tag{13}$$

In Equation (12) $\boldsymbol{C} = 0.57721566$ (Euler constant) and hyperbolic cosine and sine as well as hyperbolic cosine (sine) integrals are used. The integral in Equation (12) decreases with growth of $\widetilde{z}$ and has the following asymptotic representation (which is obtained with integration by parts):

$$\int_0^\infty \frac{u\cos(\widetilde{z}u)}{1+u^2}\,\mathrm{d}u \approx -\widetilde{z}^{-2} - 6\widetilde{z}^{-4} - 120\widetilde{z}^{-6} + \cdots \tag{14}$$

This result gives rather high precision for the value in square brackets in Equation (12) for large values of $\widetilde{z}$ (for $\widetilde{z} = 12$ the relative error $<10^{-6}$); for parameter a the error will be even smaller. For small $\widetilde{z}$ the value in square brackets in Equation (12) has the representation

$$\tfrac{1}{4}\widetilde{z}^2[3 - 2\boldsymbol{C} - 2\ln(\widetilde{z})] + \tfrac{1}{288}\widetilde{z}^4[25 - 12\boldsymbol{C} - 12\ln(\widetilde{z})] + \cdots \tag{15}$$

Denote multipliers to η in equations for a and b by S_a and S_b, respectively. Keeping in mind that a suitable determination of damping parameters is important only in the frequency interval where natural frequencies of the system lie, define parameter ε for above models stipulating that value S_b deviate from unit value less than by 3% for $z \geqslant 1$. This leads to $\varepsilon = 1/21.2, 1/4, 1/3.51$ for kernels (2), (8), (11), respectively. Going to non-dimensional frequency z, replace in equations for a and b argument $\widetilde{z}$ by $21.2z, 4z, 3.51z$ for kernels (2), (8), (11), respectively. At the first natural frequency $\omega = \omega_1$ ($z = 1$), values of S_a will be 1.945, 1.294, 1.107 for kernels (2), (8), (11) with subsequent growth for increasing z. The increase in S_a leads to a deviation of a from desired unit value. This deviation becomes too large with increase of damping parameter η and frequency z (e.g. for $\eta = 0.4$ and $z = 5$ parameter $a = 2.188, 1.938, 1.876$ for kernels (2), (8), (11) respectively instead of $a = 1$).

Besides above considered kernels with logarithmic singularity at origin, rather attractive is a kernel in the form of a sum of exponential functions. This corresponds to Maxwell–Wiechert model [23–25] which consists of a number of Maxwell elements, joined in parallel, with adding a linear elastic spring. In paper [15] by Makris and Zhang the similar treatment is applied for approaching the Biot model. Because of logarithmic singularity in the Biot kernel, a good approximation with a sum of few exponential functions is difficult. In an example [15], approximation for damping coefficient b contains an error about 15%. More appropriate is a direct application of the Maxwell–Wiechert model for frequency domain approximation omitting the Biot model. The function G in Equation (4) with $\varepsilon = 1$ is represented in the form (Prony series):

$$G(\varepsilon(\tau - s)) = \sum_{j=1}^{N} k_j \exp(-\gamma_j(\tau - s)) \tag{16}$$

DOI: 10.1002/eqe

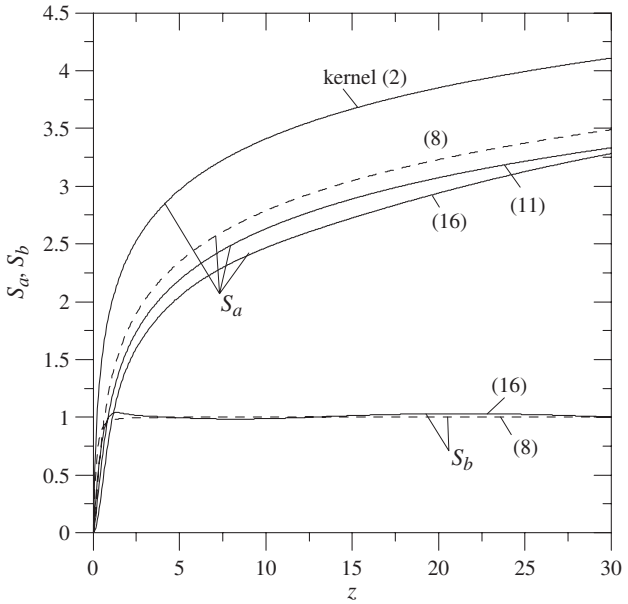

Figure 1. Normalize stiffness for hereditary models.

where k_j, γ_j are non-dimensional parameters. Values a and b entering complex stiffness k^* in Equation (5) will be

$$a = 1 + \eta S_a, \quad S_a = \sum_{j=1}^{N} k_j \frac{z^2}{\gamma_j^2 + z^2} \tag{17}$$

$$b = \eta S_b, \quad S_b = \sum_{j=1}^{N} k_j \frac{z\gamma_j}{\gamma_j^2 + z^2} \tag{18}$$

Suppose it is required to ensure nearly constancy of S_b, i.e. $S_b = 1$, at the frequency interval $1 \leqslant z \leqslant 30$. Taking $N = 4$, $\gamma_1 = 0.9$, $\gamma_2 = 4.5$, $\gamma_3 = 12.5$, $\gamma_4 = 30$ and requiring unit values of S_b at $z = \gamma_j$, we obtain (solving the corresponding system of linear equations) $k_j = 1.55394, 0.878069, 0.0941176, 1.58239$ for $j = 1, 2, 3, 4$ respectively. It is appropriate to take the found values of k_j with the multiplier 0.99 for diminishing Δ—maximum deviation S_b from 1 at the considered frequency interval; Δ becomes less than 3% (as above for the logarithmic kernels). After frequency $z = 30$, a slow decrease in S_b takes place. Note that $S_a(1) = 0.8932$ (with considering above correction). The values of parameters γ_j (the inverses of the relaxation times of the Maxwell elements) can be arbitrary to a certain extent but providing positive values of k_j; it is appropriate to take the first and last values equal approximately to z interval boundaries and to crowd other γ_j points to the left bound of the z interval using a geometric progression for $\gamma_{j+1} - \gamma_j$. Values S_a and S_b are shown in Figure 1; also in Figure 1 the values for kernels (2), (8), (11) are represented. For chosen accuracy (3%) of approximation of the unit value by function S_b, we have nearly the same quality of approximation relating to S_a for kernels (11) and (16) and somewhat worse

DOI: 10.1002/eqe

approximation for kernels (8) and (2). Besides more acceptable behaviour of the function S_a (i.e. more nearness to zero), application of the kernel (16) has the following important advantage as compared with kernels having logarithmic singularity: when numeric integrating the corresponding system of equations for the studied mechanical system, the structure of the kernel does not require the remembering all previous values of $\dot{x}$; one can deal with accumulated values of integrals containing $\dot{x}$ multiplied by $\exp(\gamma_j s)$ (see Equations (4), (16)).

Sacrificing the accuracy in static stiffness, one can improve the quality of approximation for the real part of the normalized complex stiffness for the frequency interval containing natural frequencies of the system. Clearly this interval is most important when studying transient vibrations. Instead of Equation (4) consider the equation:

$$F = k\left[\beta x + \eta \int_0^{\tau} G(\varepsilon(\tau - s))\frac{\mathrm{d}x}{\mathrm{d}s}\,\mathrm{d}s\right] \tag{19}$$

where a positive coefficient $\beta<1$ is introduced. In Equations (6), (9), (12), (17) for parameter a the addendum 1 is changed to β. Define β requiring that for $z=1$

$$a = 1 \tag{20}$$

We obtain from Equation (20) the following equation for β:

$$\beta = 1 - \eta S_a(1) \tag{21}$$

where the non-dimensional frequency z as the argument in S_a is considered. According to above results $S_a(1) = 1.945, 1.294, 1.107, 0.8932$ for kernels (2), (8), (11), (16) respectively. Using Equations (19), (21) we obtain the correct value of a at the first natural frequency and reduced errors for $z>1$. The underestimation of the static stiffness, βk, will be not important if the main interest lies in the study of transient processes.

CAUSAL MODEL BASED ON APPLICATION OF IMAGINARY PART OF WHOLE COMPLIANCE FOR BUILDING TRANSIENT RESPONSE OF MECHANICAL SYSTEM

In this section, a causal linear model with nearly constant stiffness is constructed for a mechanical system considered as a whole. Let $X(\omega) + \mathrm{i}Y(\omega)$ be complex compliance for an element of a linear causal system. It is assumed that steady-state complex amplitude $X(\omega)+\mathrm{i}Y(\omega)$ corresponds to the load $\exp(\mathrm{i}\omega t)$ acting in a point of the system or to a group of such loads applied in different points. From the linearity follows that the real function $X(\omega)$ should be symmetric relative to the point $\omega=0$, and the function $Y(\omega)$ is anti symmetric. Using these properties and taking into account that Dirac δ-function has the representation:

$$\delta(t) = \frac{1}{2\pi}\int_{-\infty}^{\infty} \exp(\mathrm{i}\omega t)\,\mathrm{d}\omega \tag{22}$$

we obtain the following equation for the response of the considered element upon instantaneous unit impulse (i.e. δ-function):

$$U(t) = \frac{1}{\pi}\int_0^{\infty} [X(\omega)\cos(\omega t) - Y(\omega)\sin(\omega t)]\,\mathrm{d}\omega \tag{23}$$

DOI: 10.1002/eqe

Since for negative values of t this function should be equal to zero, the following relationship results (for arbitrary positive t):

$$\int_0^\infty X(\omega)\cos(\omega t)\,\mathrm{d}\omega = -\int_0^\infty Y(\omega)\sin(\omega t)\,\mathrm{d}\omega \tag{24}$$

This leads to ($t>0$)

$$U(t) = -\frac{2}{\pi}\int_0^\infty Y(\omega)\sin(\omega t)\,\mathrm{d}\omega \tag{25}$$

Note that from Equation (24) follows well-known representation of $X(\omega)$ through $Y(\omega)$ and vice versa in the form of Hilbert transformation (see References [26–28]). Equation (25) can be effectively used for calculations due to rapid convergence of the integral when inertial properties of the mechanical system are taken into account. For a system with masses and approximately constant stiffness and damping characteristics, the value $Y(\omega)$ decreases as ω^{-4} for large values of ω ($\omega>\omega_h$, where ω_h is the highest taken into account natural frequency of the system). For loads with arbitrary common time variation acting in the same points where the impulses are applied the corresponding result is obtained using superposition principle, i.e. by suitable integration (Duhamel integral) under integral in Equation (25). For non-dimensional time τ and non-dimensional frequency z introduced above, Equation (25) takes the form ($\tau>0$)

$$U(\tau) = -\frac{2\omega_1}{\pi}\int_0^\infty Y(z)\sin(z\tau)\,\mathrm{d}z \tag{26}$$

An efficient method for study transient vibrations of a mechanical system with approximately constant (frequency independent) damping and stiffness properties can be developed using Equations (26) in which, while constructing $Y(z)$, for all 'springs' entering the mechanical system the equation of the type (5) is applied with

$$a = 1, \quad b = \eta\frac{z^3}{q^3 + |z|^3} \tag{27}$$

where different values of η can correspond to different 'springs', and q is a small positive parameter, e.g. $q = 0.25$. Certainly, other similar expressions for b are acceptable. Zero b value at $z = 0$ is desirable since this excludes a discontinuity (e.g. taking place if we take $b = \eta$) when going into domain of negative frequencies and therefore excludes an unbound growth (nearly the point $z = 0$) in the real part of the complex compliance which is defined by Hilbert transformation applied to $Y(z)$. Actually, besides domain of small frequencies, the constructed value of Y practically coincides with that corresponding to strictly constant complex stiffness of 'springs'. The discrepancies in the small frequency domain lead to noticeably different responses only for large values of time. So, for a constant acting force we obtain the unbounded growth of displacements with time in the case $b = \eta$ and tending to a limit (slightly exceeding the corresponding static stiffness) in the case of Equation (27). Due to application of expression (26) for $\tau>0$ the problem of non-causality is expelled. The corresponding real part of the complex compliance, not needed for studying transient vibrations using Equation (26), can be found with the help of Hilbert transformation [26–28]. For $z>0$:

$$X(z) = -\frac{1}{\pi}\int_0^\infty \frac{Y(x)}{x+z}\,\mathrm{d}x - \frac{1}{\pi}P.V.\int_0^\infty \frac{Y(x)}{x-z}\,\mathrm{d}x \tag{28}$$

DOI: 10.1002/eqe

where the denotation of Cauchy principal value is used. Here argument x is put instead of z in $Y(z)$. Note again rapid convergence of integrals for large x values (after an interval containing natural frequencies of the system). When applying Equation (26) for the hereditary models considered in the previous section we use the found values of a and b while constructing Y. For very small values of η they are close to given in Equation (27) at the interval $1 \leqslant z \leqslant z_h = \omega_h/\omega_1$, therefore the corresponding whole compliances also will be close. Calculations show that the suggested methods (26) and (27) leads to acceptable results also in the cases when damping parameters exceed the value limiting the application of the hereditary models. Note that applying Equations (26)–(28) in a general case, we have no possibility to define the final properties of individual stiffness and damping elements entering the considered mechanical system (for the system with one degree of freedom, such determination can be made which is shown in the next section); we deal with the system as a whole. This situation is similar to that corresponding to the method of equivalent viscous damping in which giving specific damping coefficients (influenced of masses of the system) to different modes of vibrations, we lose a direct connection with individual material parts ('springs') of the considered system.

EXAMPLES OF CALCULATIONS

System with one degree of freedom

Let a system have one degree of freedom with $\omega_1 = \omega_h = (k/M)^{1/2}$ where M is the mass of the system. It is interesting to compare complex compliances of the whole system for 5 models: (1) proposed in the previous section in Equations (26), (27); (2) corresponding to the constant complex stiffness $k^* = k(1 + \mathrm{i}\eta)$; (3) corresponding to the model of equivalent viscous damping with $k^* = k(1 + \mathrm{i}z\eta)$; (4) Biot models (6), (7); (5) models (19), (16) with the corresponding value of β (21). The imaginary parts of compliances for these models $Y_j(z)$ $(j = 1, \ldots, 5)$ are defined by the equation

$$Y(z) = -\frac{1}{k}\frac{b}{(a - z^2)^2 + b^2} \tag{29}$$

with suitable values for a and b: by Equation (27) with $q = 0.25$ for $Y_1(z)$; $a = 1$, $b = \eta$ for $Y_2(z)$; $a = 1, b = \eta z$ for $Y_3(z)$; by Equations (6) and (7) with $\widetilde{z} = 21.2z$ for $Y_4(z)$; by Equations (17), (18) with $a = \beta + \eta S_a$, $N = 4$ and parameters k_j, γ_j found above, for $Y_5(z)$. Values of $Y_j(z)$ $(j = 1, 2, 3, 5)$ are close to each other in a vicinity of the resonance frequency $z = 1$ and for large values of z (Figure 2), discrepancies are noticeable only for large values of η in the area of small z. In the behaviour of $Y_4(z)$ the influence of increase in a with frequency growth is evident. Consider real parts of the compliances. For the first model $X_1(z)$ is defined according to Equation (28) using $Y_1(z)$, and for the rest of models the following equation is applied:

$$X(z) = \frac{1}{k}\frac{a - z^2}{(a - z^2)^2 + b^2} \tag{30}$$

with corresponding values of a and b. Values $kX(z)$ for the models are represented in Figure 3 for $\eta = 0.2, 0.4$. Note a noticeable increase in the static compliance for hereditary model 5 using parameter β and non-significant such increase for model 1, with growth of damping. For small values of η ($\eta < 0.1$) all the functions (except $X_4(z)$) are very close.

DOI: 10.1002/eqe

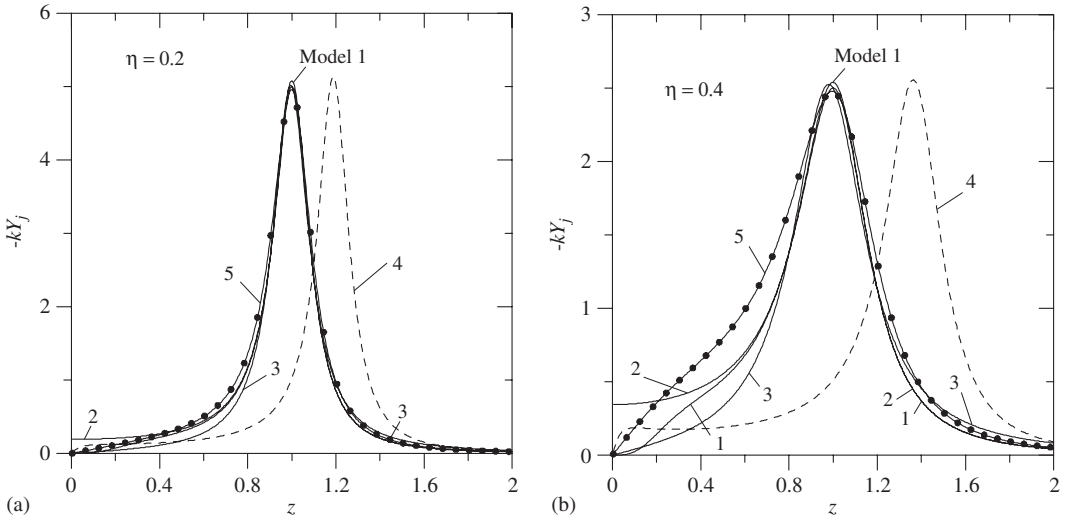

Figure 2. Imaginary part of SDoF compliance for five models at damping parameter: (a) $\eta = 0.2$; and (b) 0.4.

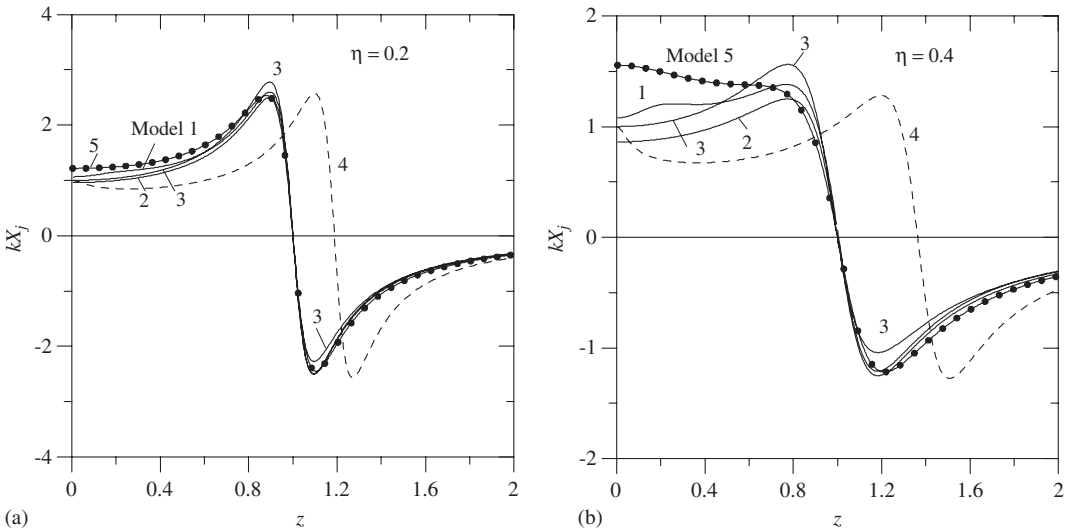

Figure 3. Real part of SDoF compliance for five models at damping parameter: (a) $\eta = 0.2$; and (b) 0.4.

Defining for model 1 the total complex stiffness $X(z) + \mathrm{i}Y(z)$ with the help of Equations (29), (28) one can raise the question: to which stiffness of the spring this total stiffness corresponds? Denoting the normalize stiffness of the spring as $\widetilde{a} + \mathrm{i}\widetilde{b}$ we obtain the following system of equations

DOI: 10.1002/eqe

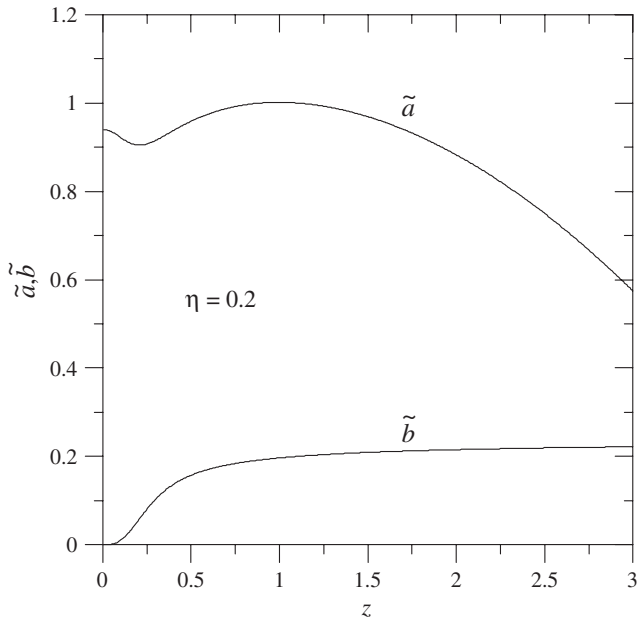

Figure 4. Recovery of normalized spring stiffness for model 1.

for $\tilde{a}$ and $\tilde{b}$:

$$\frac{\tilde{a} - z^2}{(\tilde{a} - z^2)^2 + \tilde{b}^2} = kX(z) \tag{31}$$

$$\frac{\tilde{b}}{(\tilde{a} - z^2)^2 + \tilde{b}^2} = -kY(z) \tag{32}$$

This system leads to

$$\tilde{b} = -\frac{kY(z)}{[kX(z)]^2 + [Y(z)]^2} \tag{33}$$

$$\tilde{a} = z^2 + \frac{kX(z)}{[kX(z)]^2 + [Y(z)]^2} \tag{34}$$

Values $\tilde{a}$ and $\tilde{b}$ are represented in Figure 4 for $\eta = 0.2$. For $z = 1$ they are: $\tilde{a} = 1.0014$, $\tilde{b} = 0.1969$, i.e. very close to the required values. With increase of z the deviation of $\tilde{a}$ from 1 grows, however the value $\tilde{a} - z^2$, which is used actually when calculating the stiffness, is close to the desired value $1 - z^2$; this fact is proved also by a proximity of the results for models 1 and 2 given in Figure 3.

Consider responses of above models upon instantaneous unit impulse. Using Equations (26), (29) represent function $U(\tau)$ in the form

$$U(\tau) = \frac{2}{\sqrt{kM}\pi} \int_0^\infty \frac{b}{(a - z^2)^2 + b^2} \sin(z\tau)\, \mathrm{d}z \tag{35}$$

DOI: 10.1002/eqe

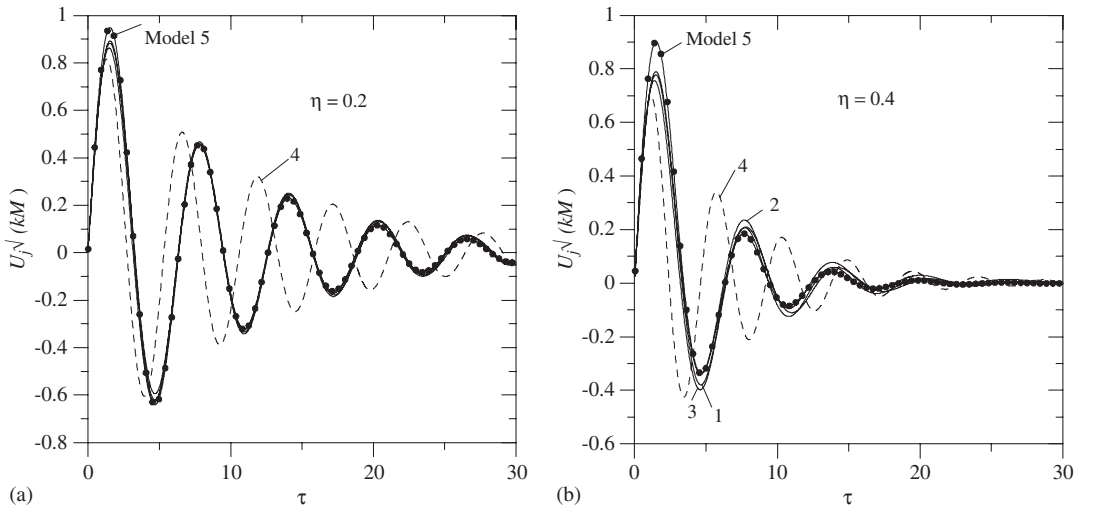

Figure 5. Response of SDoF on instantaneous impulse for five models at damping parameter: (a) $\eta = 0.2$; and (b) 0.4.

with a and b determined above for each model. Certainly, for the third model (equivalent viscous) the simpler expression can be used:

$$U(\tau) = \frac{\exp(-0.5\eta\tau)}{\sqrt{kM}\sqrt{1-\eta^2/4}} \sin\left(\tau\sqrt{1-\eta^2/4}\right) \tag{36}$$

We keep name 'model with constant complex stiffness' for the second model although applying Equations (26), (29) for $a = 1$, $b = \eta$ we make the model causal assuming that the real part of the whole compliance is defined according to Equation (28) (not by Equation (30)); actually under the name 'model 2' now another model is dealt. The values of $(kM)^{1/2}U(\tau)$ for the five models are shown in Figure 5 for $\eta = 0.2, 0.4$. Note non-significant discrepancies between results for models 1, 2, 3, 5 even for $\eta = 0.4$; without the correction by introducing parameter β, Biot kernel (model 4) leads to significant deviations from the results predicted by other models.

The case of constant unit force applied to the system at moment $t = 0$ reveals noticeable differences in large time responses for the models because of differences in real parts of compliances for small frequencies. We use instead of Equation (26) the equation:

$$U(\tau) = \frac{2}{k\pi}\int_0^\infty \frac{b}{(a-z^2)^2+b^2}\frac{1-\cos(z\tau)}{z}\,\mathrm{d}z \tag{37}$$

The convergence of the integral becomes even better. It can be shown that for $b(0) \neq 0$ (as in the case of the Model 2), this integral increases logarithmically with $\tau \to \infty$. The results for the five models are shown in Figure 6. For large values of τ and η the hereditary model with parameter β (fifth) and the second model (with constant stiffness but made causal) lead to noticeable overstating displacements according to overstating the compliance for small frequencies. For the second model displacements increase without limit, whereas for the fifth model the limiting value equals with high precision the value $1/(k\beta)$ which gives a good confirmation for correctness of calculations.

DOI: 10.1002/eqe

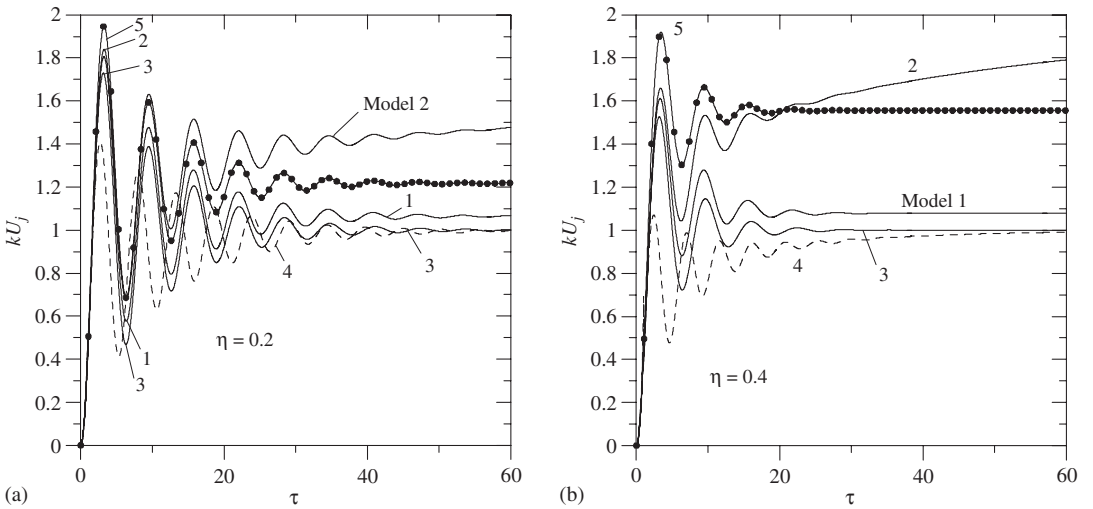

Figure 6. Response of SDoF on sudden application of constant force for five models at damping parameter: (a) $\eta = 0.2$; and (b) 0.4.

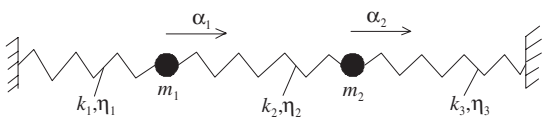

Figure 7. Example of two degree of freedom system.

The correction for b made in Equation (27) results in adequate behaviour of the first model even for large time values and large values of damping coefficients η. The normalized limiting values of displacements for this model are 1.039, 1.064, 1.079 for $\eta = 0.1, 0.2, 0.4$ respectively; these values equal the corresponding values of $kX_1(0)$. For models 3 and 4 the normalized limiting values equal one.

Summarizing note that the two models—first and third—are rather close in the all above examples. The hereditary model 4 leads to a shifting of the resonance frequency which is exhibited in all examples. This fault is excluded in model 5, however the diminishing the static stiffness can result in an erroneous longtime response as in the example with the constant acting force. The causal model corresponding to model 2 also leads to inadequate longtime response; in the case of constant force displacements increase without limit with increase of time.

System with two degrees of freedom

Further, we analyse the case of a system having more than one degree of freedom when advantages and shortcomings of the models are seen more explicitly. Consider a system (Figure 7) consisting of equal masses $m_1 = m_2 = M$ connected with springs having stiffness $k_1 = k_2 = k_3 = k$ and damping parameters $\eta_1 = \eta_2 = \eta_0, \eta_3 = 0$. Masses and stiffness are distributed symmetrically whereas damping properties are non-symmetric. In this example, some incorrectness of the equivalent

DOI: 10.1002/eqe

viscous damping method, which impose modes of the symmetric undamped system on the given non-symmetrical system, can be demonstrated. The natural frequencies are

$$\omega_1 = \sqrt{\frac{k}{M}}, \quad \omega_2 = \omega_1\sqrt{3} \tag{38}$$

Consider complex compliances for masses corresponding to two forces: $\exp(\mathrm{i}\omega t)$ applied to the mass m_1 and $-\exp(\mathrm{i}\omega t)$ applied to the mass m_2. Denote α_1 and α_2 complex amplitudes for masses m_1 and m_2 respectively. The system of equations for these values has the following form:

$$-z^2\alpha_1 + (a + \mathrm{i}b)\alpha_1 + (a + \mathrm{i}b)(\alpha_1 - \alpha_2) = \frac{1}{k} \tag{39}$$

$$-z^2\alpha_2 + \alpha_2 - (a + \mathrm{i}b)(\alpha_1 - \alpha_2) = -\frac{1}{k} \tag{40}$$

where a and b have different determinations for the different considered models 1, 2, 4, 5 (see the description after Equation (29) where $\eta = \eta_0$). While using the method of equivalent viscous damping (model 3) we study a symmetrical motion, i.e. the motion of a one degree of freedom system with mass M and complex stiffness

$$k^* = 3k(1 + \mathrm{i}\widetilde{\eta}z/\sqrt{3}) \tag{41}$$

where

$$\widetilde{\eta} = \frac{\eta_1 + 4\eta_2}{6} = \frac{5}{6}\eta_0 \tag{42}$$

The coefficient $\widetilde{\eta}$ is found using the requirement that for each mass in a symmetrical harmonic motion at frequency $z = 3^{1/2}$, loss of energy equals the half of total loss of energy for the given system in the motion. In Figure 8 values $k|\alpha_1|$ and $k|\alpha_2|$ for second and third models are shown for the given symmetrical loading. The method of equivalent viscous damping (third model) results in identical amplitudes of masses. For the second model the amplitudes of masses are different; at $z = 1$ the first mass has zero amplitude and the amplitude of the second mass is about twice as great as the result for the equivalent viscous model. This model is unacceptable near the first resonance frequency for the considered loading.

Further consider imaginary parts $Y(z)$ of the complex compliance of the first mass for the five models described above in the case of the given symmetrical loading. For models 1, 2, 4, 5, Equations (39), (40) are used with suitable values of a and b, and $Y(z) = \mathrm{Im}(\alpha_1)$. For the third model, the mass M attached to a spring with stiffness (41) is considered. In Figure 9 the corresponding results are shown. We observe again the behaviour of the equivalent viscous model differing from that for other models. At the first natural frequency ($z = 1$) values Y are zero for all the models except model 3. For the two hereditary models, especially for model 4, the shift of resonance frequencies because of growth of parameter a is to be noted. The application of parameter β in the model 5 softens this phenomenon. Consider real parts $X(z) = \mathrm{Re}(\alpha_1)$ of the complex compliance for the models described above in the case of the given symmetrical loading. For the model 2, 4, 5 we use directly the relationship $X(z) = \mathrm{Re}(\alpha_1)$, for the first model Equation (28) is applied using already discussed value $Y(z)$ and for the third model the above simple system is considered. The shortcomings of models 3, 4, 5 are seen also in Figure 10 where the values $kX(z)$ are represented. For models 2, 4, 5 value of $kX(1) = 0$ whereas for model 1 this value is

DOI: 10.1002/eqe

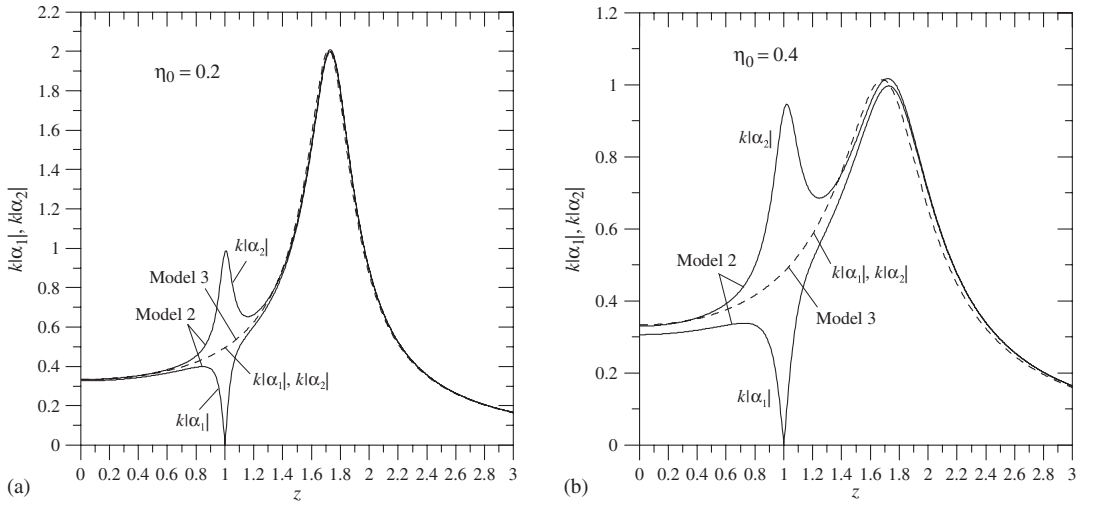

Figure 8. Example on incorrect amplitudes prediction by equivalent viscous model at damping parameter: (a) $\eta = 0.2$; and (b) 0.4; system of Figure 7 is loaded symmetrically by two harmonic forces.

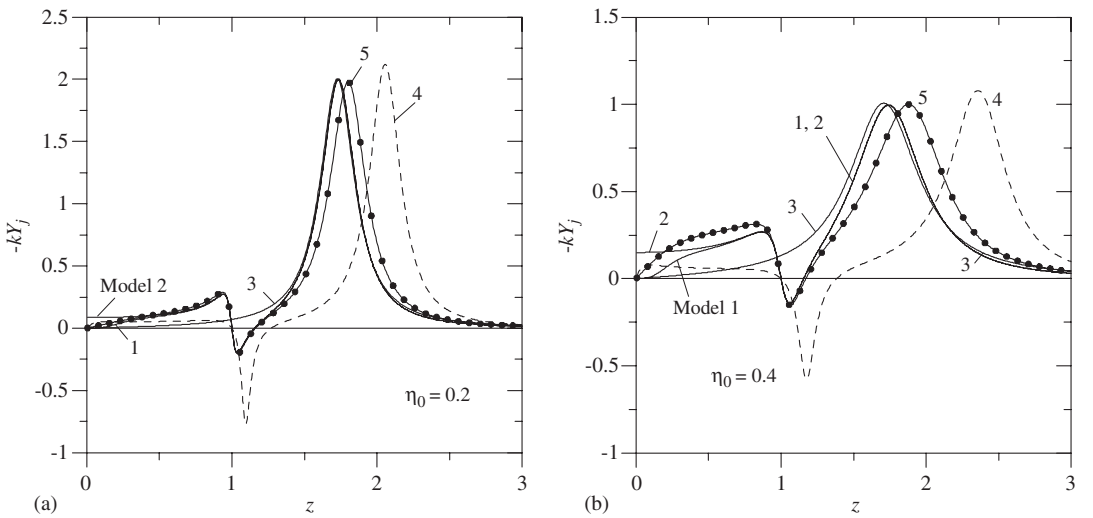

Figure 9. Imaginary part of compliance for two degree of freedom system for five models at damping parameter: (a) $\eta = 0.2$; and (b) 0.4; system of Figure 7 is loaded symmetrically by two harmonic forces.

equal about 1.3η and for the third model $kX(1) \approx 0.48$ which differs sharply from the results for other models.

It interesting to study transient vibrations of mass m_1 when two symmetrical forces $\sin(\omega_1 t)$ and $-\sin(\omega_1 t)$ are applied to masses m_1 and m_2, respectively. The frequency of excitation equals the first natural frequency of the given mechanical system. In order to obtain equation of motion for the mass m_1, one can use values $Y(z)$ considered above and integrate by s the function

DOI: 10.1002/eqe

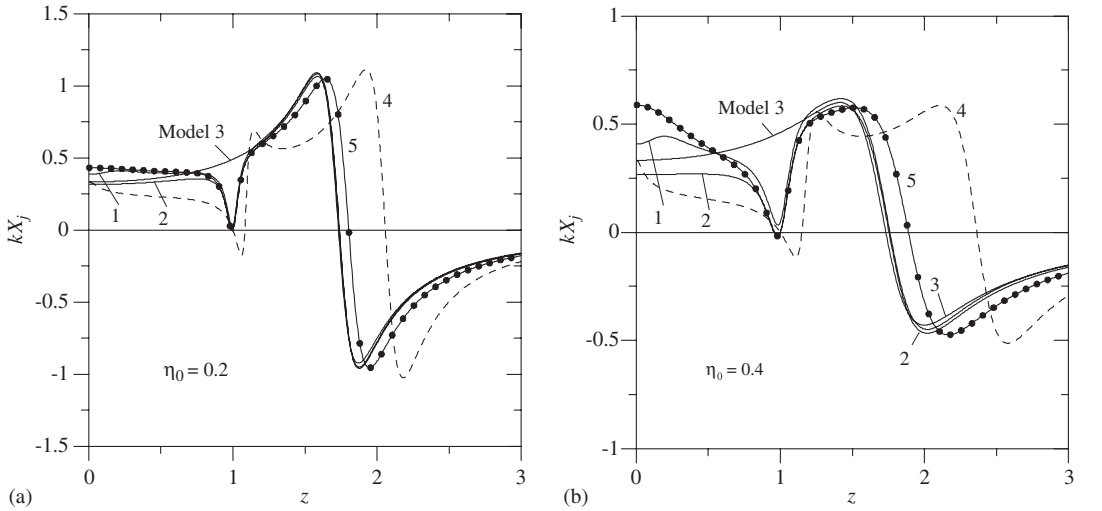

Figure 10. Real part of compliance for two degree of freedom system for five models at damping parameter: (a) $\eta = 0.2$; and (b) 0.4; system of Figure 7 is loaded symmetrically by two harmonic forces.

$\sin[z(\tau - s)]\sin(s)/\omega_1$ from 0 to τ under integral sign in Equation (26). The equation of motion of the first mass has the form:

$$U(\tau) = -\frac{2}{\pi}\int_0^\infty Y(z)\frac{z\sin(\tau) - \sin(z\tau)}{z^2 - 1}\,\mathrm{d}z \tag{43}$$

For $z \to 1$, the limit of the multiplier to $Y(z)$ equals $0.5[\sin(\tau) - \tau\cos(\tau)]$. The results of calculations for $\eta = 0.4$ are shown in Figure 11. The displacements corresponding to model 3 (equivalent viscous) become steady state after several oscillations; the amplitude of vibrations equals the amplitude for $z = 1$ in Figure 8 with high precision. For other models, the amplitudes decrease accordingly to their steady-state values (zero for models 2, 4, 5 and a small value for model 1).

Vibrations of shear beam

Consider a vertical shear beam with fixed bottom section having unit cross-section area with complex shear modulus $G = G_0(a + \mathrm{i}b)$ and density ρ under action of the lateral volume load $\exp(\mathrm{i}\omega t) = \exp(\mathrm{i}z\tau)$ with unit amplitude. Let H be the length of the beam and location of beam points is defined by co-ordinate y measured from the beam bottom. Such a system is of importance when studying shear wave propagation through deformable medium. Natural frequencies of the beam (for $G = G_0$) are

$$\omega_j = \frac{\pi(2j-1)}{2H}\sqrt{\frac{G_0}{\rho}} \quad (j = 1, 2, \ldots) \tag{44}$$

with the following corresponding modes of vibrations:

$$w_j(\gamma) = \sin\left(\frac{2j-1}{2}\pi\gamma\right) \tag{45}$$

DOI: 10.1002/eqe

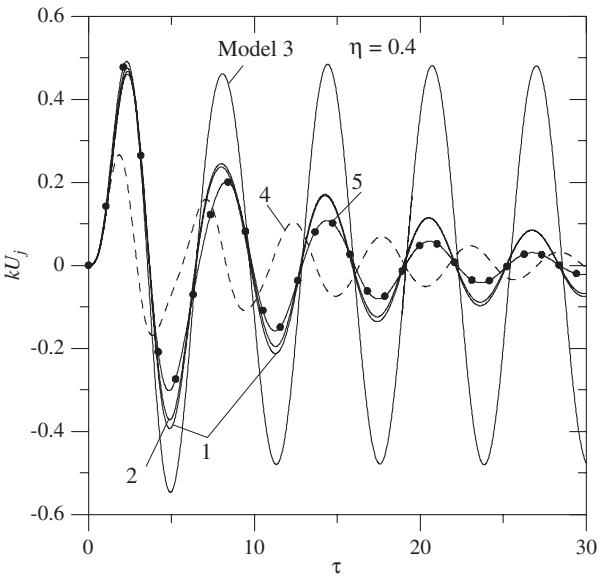

Figure 11. Transient response of two degree of freedom system of Figure 7 loaded symmetrically by two sinusoidal forces.

where

$$\gamma = \frac{y}{H} \tag{46}$$

As above the frequency ω_1 is used for determination of $z = \omega/\omega_1$. Steady-state complex amplitudes of lateral vibrations of the beam will be

$$u_0(y) = \frac{1}{\rho\omega^2}[\cos(\lambda y) + \sin(\lambda y)\tan(\lambda H) - 1] \tag{47}$$

where

$$\lambda = \omega\sqrt{\frac{\rho}{G_0(a + \mathrm{i}b)}} \tag{48}$$

Or

$$u_0(y) = \frac{1}{\rho\omega_1^2 z^2}\left[\cos\left(\frac{\pi z\gamma}{2\sqrt{a + \mathrm{i}b}}\right) + \sin\left(\frac{\pi z\gamma}{2\sqrt{a + \mathrm{i}b}}\right)\tan\left(\frac{\pi z}{2\sqrt{a + \mathrm{i}b}}\right) - 1\right] \tag{49}$$

The imaginary part of the compliance, $Y(z)$, for the point $y = H$ has the form:

$$Y(z) = \frac{1}{\rho\omega_1^2 z^2}\mathrm{Im}\left(1/\cos\frac{\pi z}{2\sqrt{a + \mathrm{i}b}}\right) \tag{50}$$

This results in the following expression relating to the endpoint acceleration:

$$Y_a(z) = -\frac{1}{\rho}\mathrm{Im}\left(1/\cos\frac{\pi z}{2\sqrt{a + \mathrm{i}b}}\right) \tag{51}$$

DOI: 10.1002/eqe

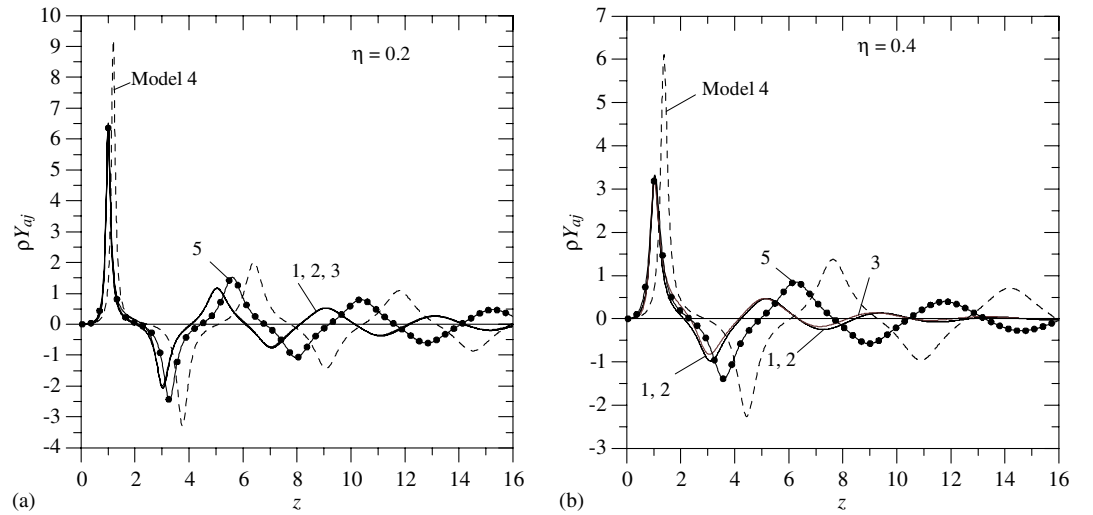

Figure 12. Imaginary part of acceleration amplitude at top of beam for five models at damping parameter: (a) $\eta = 0.2$; and (b) 0.4.

Equations (50), (51) with appropriate values of a and b is used for models 1, 2, 4, 5: for model 1, a and b are defined by Equation (27); for model 2, $a = 1$, $b = \eta$; for model 4, by Equations (6) and (7) with $\tilde{z} = 21.2z$; for model 5, by Equations (17), (18) with $a = \beta + \eta S_a$, $N = 4$ and parameters k_j, γ_j found above. For the model 3 (equivalent viscous), one can consider the series expansion of Equation (49) using the modes (45) and taking for the modes $a + \mathrm{i}b = 1 + \mathrm{i}\eta z/(2j - 1)$. This ensures for the material the same damping parameter, η, at natural frequencies $z_j = 2j - 1$. We obtain instead of Equation (49)

$$u_0(y) = \frac{4}{\pi\rho\omega_1^2} \sum_{j=1}^{\infty} \frac{w_j(\gamma)}{2j-1} \frac{1}{(2j-1)^2 - z^2 + \mathrm{i}\eta z(2j-1)} \tag{52}$$

The corresponding value for the endpoint acceleration will be (instead of Equation (51))

$$Y_a = \frac{4\eta z^3}{\pi\rho} \sum_{j=1}^{\infty} \frac{(-1)^{j+1}}{[(2j-1)^2 - z^2]^2 + \eta^2 z^2 (2j-1)^2} \tag{53}$$

Note that according to Equation (52), modal damping parameters increase with growth of numbers of modes whereas the material coefficient of damping is kept constant. The function $Y_a(z)$ by Equation (53) for model 3 and by Equation (51) for model 1, 2, 4, 5 is represented in Figure 12. The values Y_a for models 1, 2, 3 practically coincide (unlike the previous examples, now they are close also for small frequencies tending to zero for $z \to 0$). The results for models 4, 5 deviate significantly from those for other models; beside the shift for resonance frequencies, larger resonance amplitudes are observed. We see that the increase in the real part of stiffness leads to diminishing the system damping although the damping parameter, b, does not change practically with frequency.

DOI: 10.1002/eqe

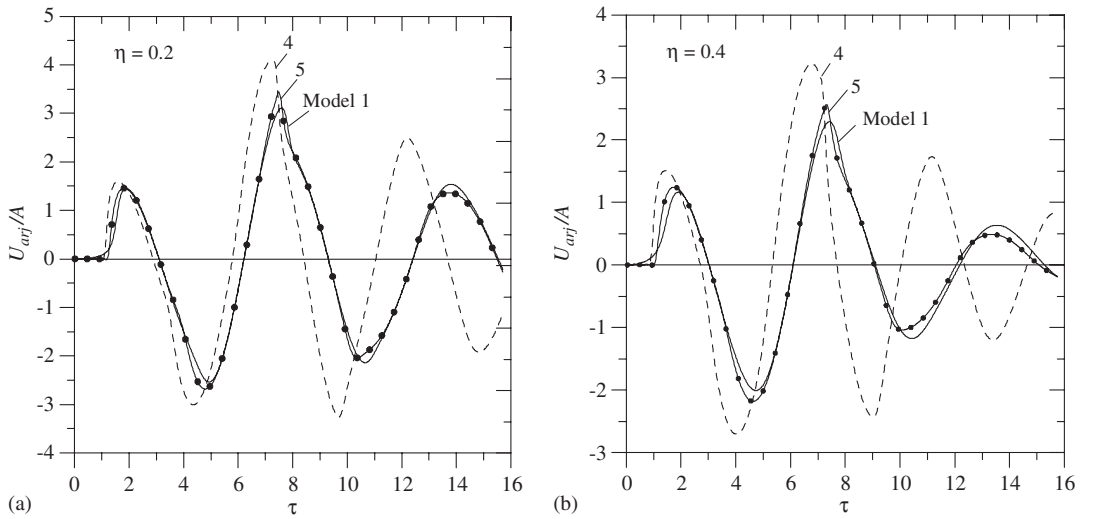

Figure 13. Relative acceleration history at top of beam excited by bottom motion with accelerogram (56) for $\Omega = 1$ at damping parameter: (a) $\eta = 0.2$; and (b) 0.4.

If the bottom of the beam moves in the transverse direction with the acceleration $f(\tau)$, then from Equations (26), (50) the following equation results for the relative acceleration of the end point of the beam:

$$U_{\mathrm{ar}}(\tau) = \frac{2}{\pi}\int_0^\infty \rho Y_a(z) F(z,\tau)\,\mathrm{d}z \tag{54}$$

where

$$F(z,\tau) = \int_0^\tau \sin[z(\tau - s)] f(s)\,\mathrm{d}s \tag{55}$$

Consider the following function representing ground accelerations [15, 29]:

$$f(\tau) = \begin{cases} A\cos(\Omega\tau) & (0 \leqslant \tau \leqslant 2\pi/\Omega) \\ 0 & (\tau > 2\pi/\Omega) \end{cases} \tag{56}$$

where A is a reference acceleration, Ω is the non-dimensional frequency of the applied acceleration impulse. The function $F(z,\tau)$ will be

$$F(z,\tau) = \begin{cases} Az\dfrac{\cos(\Omega\tau) - \cos(z\tau)}{z^2 - \Omega^2} & (0 \leqslant \tau \leqslant 2\pi/\Omega) \\ Az\dfrac{\cos[(2\pi/\Omega - \tau)z] - \cos(z\tau)}{z^2 - \Omega^2} & (\tau > 2\pi/\Omega) \end{cases} \tag{57}$$

Further consider two examples: $\Omega = 1$ and 3, i.e. the frequency of the impulse equals the first and the second natural system's frequency. Since values Y_a for models 1, 2, 3 are very close, compare endpoint accelerations only for three models: 1, 4, 5. This is done in Figures 13 ($\Omega = 1$)

DOI: 10.1002/eqe

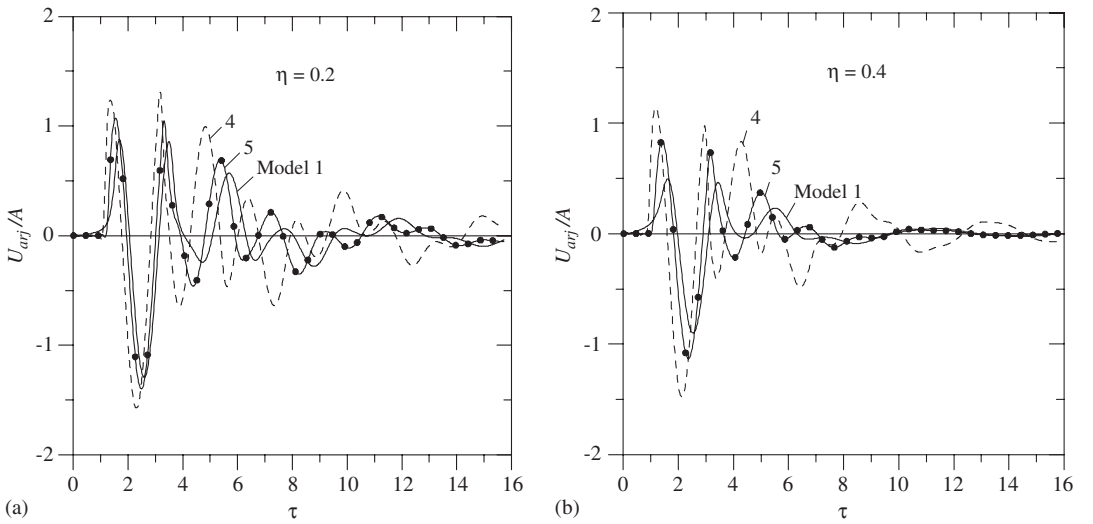

Figure 14. Relative acceleration history at top of beam excited by bottom motion with accelerogram (56) for $\Omega = 3$ at damping parameter: (a) $\eta = 0.2$; and (b) 0.4.

and 14 ($\Omega = 3$). The results for model 5 are in some proximity to that for model 1 in the case $\Omega = 1$ which corresponds to the proximity of values Y_a for these models in vicinity of the first natural frequency (Figure 12). This does not take place in the case $\Omega = 3$. In general, the behaviour of the values U_{ar} is in agreement with the behaviour of Y_a. Two facts should be noticed: (1) maximum values of accelerations are about four times larger in the first case than in the second one; (2) the double increase in the damping parameter η results in a relatively slight decrease in accelerations U_{ar}.

CONCLUSIONS

The paper is dedicated to discussion and development of questions relating to the frequency independent damping. As the concept of strictly constant complex stiffness leads to non-causality, a series of models is considered which allow an approximately constant stiffness. Well-known Biot model is supplemented with three hereditary models having properties similar to those of the Biot model. It is suggested to diminish the static stiffness of such models in order to obtain the required value of the stiffness at the first natural frequency of the given mechanical system and to compensate, at least partly, the increase in the real part of the stiffness inherent in the considered hereditary models. A new method of constructing a causal model with approximately constant stiffness is developed which allows to perform effective calculations for steady state and transient vibrations. Examples of mechanical systems having one, two and infinite degrees of freedom are studied on the basis of five models including two hereditary models, the causal model built according to the suggested method, the model relating to strictly constant stiffness which turns into the corresponding causal model when dealing with transient vibrations, and the equivalent viscous model. The latter model in majority of cases is rather acceptable, however some limitations exist

DOI: 10.1002/eqe

for its application as is shown above in the example with two degree of freedom. In addition, the determination of natural frequencies and modes in the case of large mechanical systems can be rather laborious exceeding labor inputs corresponding to the new model.

NOMENCLATURE

t	time
F	force
x	displacement
k	static stiffness
η	damping parameter (loss factor)
ε	non-dimensional scale parameter
$G(u)$	kernel in the hereditary relationship
$E_i(-u)$	exponential integral
ω	circular frequency of excitation
ω_1	the first natural (without accounting on damping) circular frequency
ω_h	the highest natural circular frequency taken into account
z	ω/ω_1, non-dimensional frequency
$\widetilde{z}$	z/ε, one more non-dimensional frequency
z_h	ω_h/ω_1, the highest non-dimensional frequency taken into account
τ	$\omega_1 t$, non-dimensional time
ka	real part of the complex stiffness (storage modulus)
kb	imaginary part of the complex stiffness (loss modulus)
$K_0(u)$	modified Bessel function
S_a, S_b	multipliers to η in equations for a and b, respectively
k_j, γ_j	parameters in Prony series expansion for the kernel G
$\beta<1$	positive coefficient for diminishing the static stiffness
$X(\omega)+\mathrm{i}Y(\omega)$	complex compliance of the whole system
$\delta(t)$	Dirac δ-function
$U(t)$	transient response of the mechanical system
M	mass of an element of the system
G	$G_0(a+\mathrm{i}b)$, complex shear modulus of the shear beam
ρ	density of the shear beam
H	length of the shear beam
$u_0(y)$	amplitude of vibration of a point with co-ordinate y
γ	y/H, relative co-ordinate of a point of the shear beam
$w_j(\gamma)$	modes of vibrations of the shear beam
U_{ar}	relative acceleration of the end point of the shear beam for ground motion

REFERENCES

1. Theodorsen T, Garrick IE. Mechanism of flutter, a theoretical and experimental investigation of the flutter problem. *NACA Report*, 1940; 685.
2. Fraijs de Veubeke BM. Influence of internal damping on aircraft resonance. *AGARD Manual on Elasticity*, vol. 1, Chapter 3, 1960.

DOI: 10.1002/eqe

3. Caughey TK. Vibration of dynamic systems with linear hysteretic damping. *Proceedings of the Fourth U.S. National Congress of Applied Mechanics*, ASME, New York, NY, 1962; 87–97.
4. Crandall SH. Dynamic response of systems with structural damping. In *Air*, *Space and Instruments*, *Draper Anniversary Volume*, Lees S (ed.). McGraw-Hill: New York, NY, 1963; 183–193.
5. Gaul L, Bohlen S, Kempe S. Transient and forced oscillations of systems with constant hysteretic damping. *Mechanics Research Communications* 1985; **12**:187–201.
6. Milne HK. The impulse response function of a single degree of freedom system with hysteretic damping. *Journal of Sound and Vibration* 1985; **100**:590–593.
7. Inaudi JA, Kelly JM. Linear hysteretic damping and the Hilbert transform. *Journal of Engineering Mechanics* (ASCE) 1995; **121**:626–632.
8. Chen JT, You DW. Hysteretic damping revisited. *Advances in Engineering Software* 1997; **28**:165–171.
9. Chen JT, You DW. An integral-differential equation approach for the free vibration of a SDoF system with hysteretic damping. *Advances in Engineering Software* 1999; **30**:43–48.
10. Inaudi JA, Makris N. Time-domain analysis of linear hysteretic damping. *Earthquake Engineering and Structural Dynamics* 1996; **25**:529–545.
11. Inaudi JA. Analysis of hysteretic damping using analytical signals. *Journal of Engineering Mechanics* (ASCE) 1997; **123**:743–745.
12. Makris N. Stiffness, flexibility, impedance, mobility and hidden delta function. *Journal of Engineering Mechanics* (ASCE) 1997; **123**:1202–1208.
13. Makris N. Causal hysteretic element. *Journal of Engineering Mechanics* (ASCE) 1997; **123**:1209–1214.
14. Biot MA. Linear thermodynamics and the mechanics of solids. *Proceedings of the Third U.S. National Congress of Applied Mechanics*, ASME: New York, NY, 1958; 1–18.
15. Makris N, Zhang J. Time domain viscoelastic analysis of earth structures. *Earthquake Engineering and Structural Dynamics* 2000; **29**:745–768.
16. Spanos PD, Tsavachidis S. Deterministic and stochastic analyses of a nonlinear system with a Biot visco-elastic element. *Earthquake Engineering and Structural Dynamics* 2001; **30**:595–612.
17. Muscolino G, Palmeri A, Ricciardelli F. Time-domain response of linear hysteretic systems to deterministic and random excitations. *Earthquake Engineering and Structural Dynamics* 2005; **34**:1129–1147.
18. Crandall SH. The role of damping in vibration theory. *Journal of Sound and Vibration* 1970; **11**:3–18.
19. Chopra AK. *Dynamics of Structures*. Prentice-Hall: Upper Saddle River, NJ, 2001.
20. Muravskii GB. On frequency independent damping. *Journal of Sound and Vibration* 2004; **274**:653–668.
21. Muravskii GB. On description of hysteretic behaviour of materials. *International Journal of Solids and Structures* 2005; **42**:2625–2644.
22. Gradsteyn IS, Ryzhik IM. *Table of Integrals, Series & Products*. Academic Press: New York, London, 1965.
23. Tschoegl N. *The Phenomenological Theory of Linear Viscoelastic Behavior*. Springer: Berlin, 1989.
24. Patlashenko I, Givoli D, Barbone P. Time-stepping schemes for systems of Volterra integro-differential equations. *Computer Methods in Applied Mechanics and Engineering* 2001; **190**(43–44):5691–5718.
25. Palmeri A, Ricciarelli F, De Luca A, Muscolino G. State space formulation for linear viscoelastic dynamic systems with memory. *Journal of Engineering Mechanics* (ASCE) 2003; **129**:715–724.
26. Papoulis A. *The Fourier Integral and its Applications*. McGraw-Hill: New York, NY, 1987.
27. Booij HC, Thoone PJM. Generalization of Kramers–Kronig transforms and some approximations of relations between viscoelastic quantities. *Rheological Acta* 1982; **21**:15–24.
28. Bracewell RN. *The Fourier Transform and its Applications*. McGraw-Hill: New York, NY, 1986.
29. Makris N. Rigidity-plasticity-viscosity: can electrorheological dampers protect base-isolated structures from near-source ground motions? *Earthquake Engineering and Structural Dynamics* 1997; **26**:571–591.

DOI: 10.1002/eqe